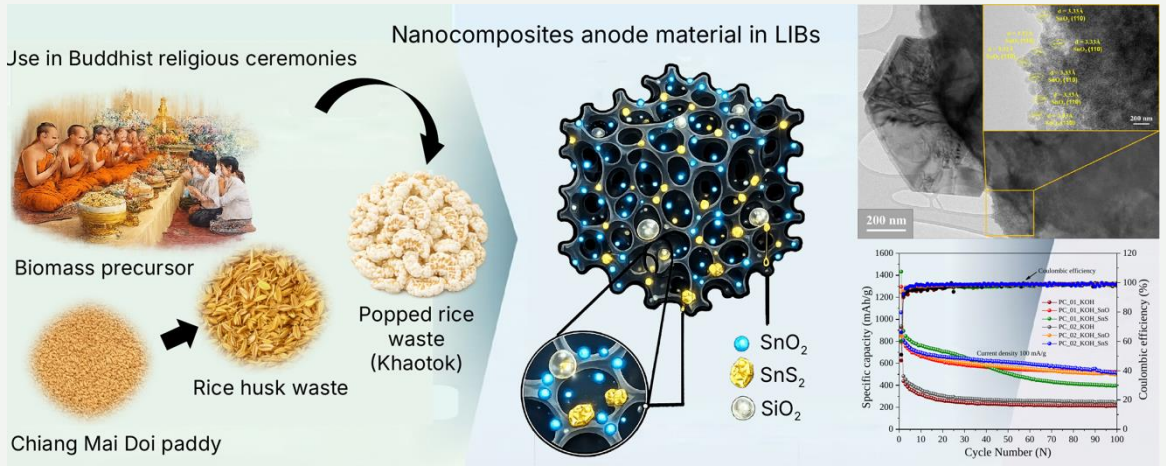
MSAT-13 | THE 4TH SYMPOSIUM ON INNOVATION AND SUSTAINABILITY

Biomass-to-Biochar for Energy Applications

Asst. Prof. Dr. Yothin Chimupala

Department of Industrial Chemistry, Faculty of Science

Chiang Mai University, Thailand



Biomass and Biochar Utilization in ASEAN Context

12 November 2026

IMPACT Exhibition and Convention Center, Muang Thong Thani

BACKGROUND AND INTRODUCTION : Li-ion Battery

Applications



- Storage capacity is determined by cathode and anode
- Drawbacks of commercial graphite: Low capacity (<372 mAh/g) and require a protection circuit for the safety batteries
- Focus on Innovative "anode materials"

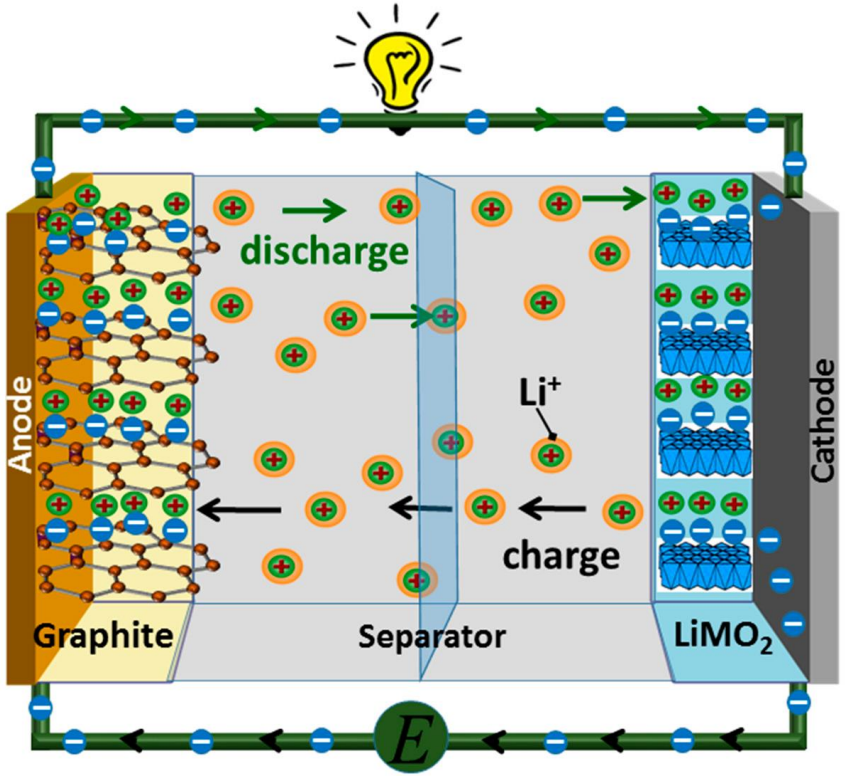


Fig 1. Schematic of the operation principles for rechargeable lithium-ion batteries.

Advantages

+ High energy density
+ Long cycle life-time
+ No memory effect
+ Low self-discharge rate
+ Long shelf-life time

Disadvantages

- High initial cost
- Safety concerns; short circuit
- Low capacity
- Slow charging

Electrochemical reaction

Anode reaction:

$$Li_xC_6 \longleftrightarrow xLi^+ + xe^- + C_6$$

Cathode reaction:

$$xLi^+ + xe^- + Li_{1-x}MO_2 \longleftrightarrow LiMO_2$$

Overall reaction:

"rocking-chair reactions"

$$LixC_6 + Li_{1-x}MO_2 \longleftrightarrow C_6 + LiMO_2$$

charging ⟷ discharging

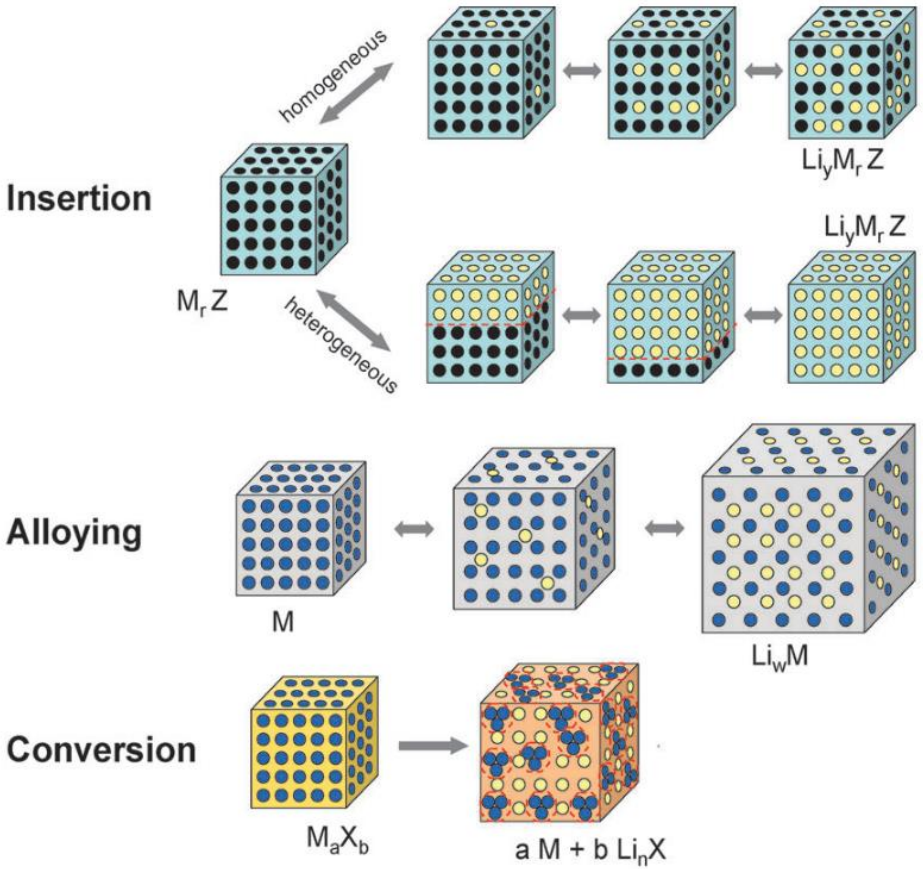
K. E. Aifantis; S. A. Hackney; R. V. Kumar, High Energy Density Lithium Batteries.: WILEY-VCH, 2010, 81, 129.]

Zubi, G. (et. al.), (2018). *Renewable and Sustainable Energy Reviews* 89: 292-308.

BACKGROUND AND INTRODUCTION: Li-ion battery

Most common anode materials used for lithium-ion batteries.

Schematic of Li^+ interaction related to volume expansion



"Usual" processes

Low capacity
(mostly limited to 1 e^- / M)

***i.e.*, Graphite, TiO_2, $Li_4Ti_5O_{12}$, Graphene**

Commercialised

Very large capacity

Volume changes are still an issue

***i.e.*, Si, Sn, Ge, Sb**
Under development

Large capacity

Voltage hysteresis

***i.e.*, Fe_2O_3, FeS_2,MnO_2**

Poor capacity retention of high-capacity electrodes

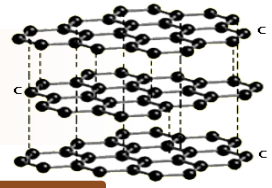
Table 1. the anode material efficiencies.

Materials	Lithiated phase	Theoretical specific capacity (mAh g^{-1})	Volume change (%)	Potential versus Li (V)
Graphite	LiC_6	372	12%	0.05
Graphene	LiC_3	744	12%	0.05-0.5
TiO_2	Li_xTiO_2	330	<4%	1.60
$Li_4Ti_5O_{12}$	$Li_7Ti_5O_{12}$	175	0.2%	1.55
Si	$Li_{4.4}Si$	4200	420%	0.40
Ge	$Li_{4.4}Ge$	1600	270%	0.50
Sn	$Li_{4.4}Sn$	994	260%	0.60
Sb	Li_3Sb	660	96%	0.30
Al	LiAl	993	96%	0.30
Mg	Li_3Mg	3350	100%	0.10
Fe_2O_3	Fe_2Li_x	1006	96%	1.60
Fe_3O_4	Fe_3Li_x	926	81.3%	1.69

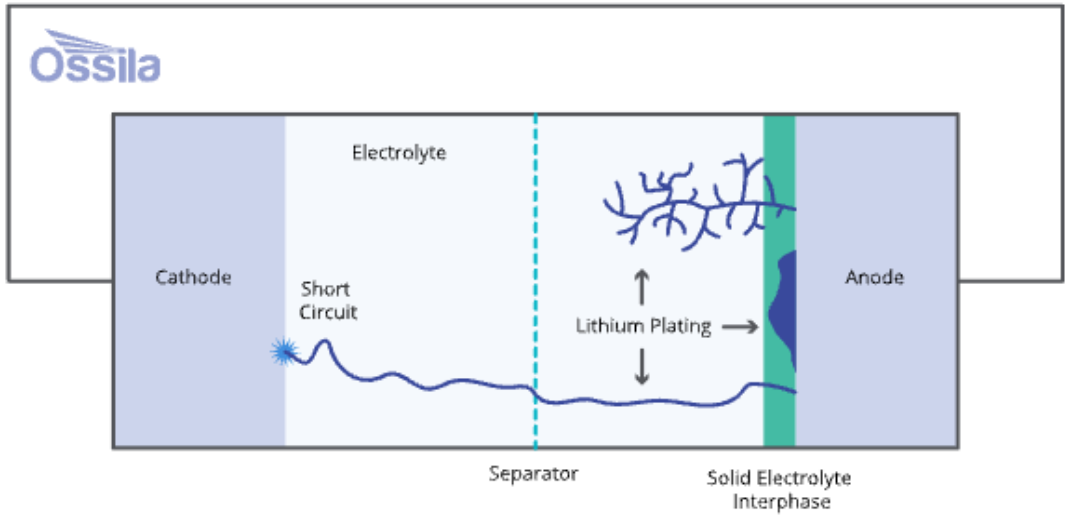
Palacín, M. R. (2009). *Chemical Society Reviews* 38: 2565–2575. Chem 4, 972–996, May 10, 2018 [a] Scrosati, B et al., Journal of Power Sources, 2010, 195, 2419. Adv. Funct. Mater. 2012,

Background and Introduction: Li-ion battery

Commercial anode: Graphite



- **Specific capacity** does not satisfy requirements **(372 mAh/g)**
- Severe structure collapse and **exfoliation over cycling** that originally starts with the formation of SEI
- **The low operating voltage of ~0.1 V vs. Li/Li^+ allows for lithium electroplating at the electrode surface.**
- At a high charging/discharging current rate, lithium dendrites can easily be formed on the graphite surface
- Dendrites can move through the separator resulting in an internal **short circuit**, cell damaging, and warming up until fire (thermal runaway).
- The use of a graphite-based anode is particularly restricted to low temperatures. (temperature range on EV -30 to +60 ºC)



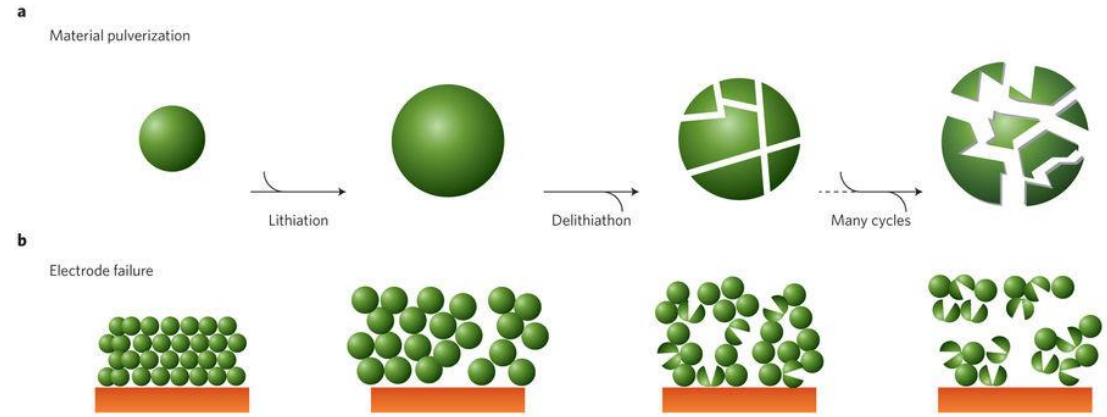
Anode Material Development

- to increase capacity
- to enhance stability of electrodes
- to improve safety in using
- to decrease production cost
- To support fast charge technologies

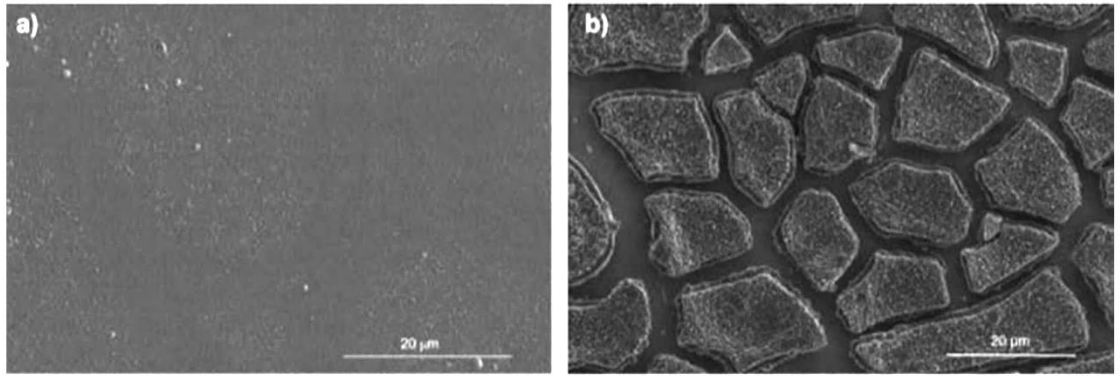
Brehob, M., et.al., (1999). *The Potential of Carbon-Based Memory Systems*. 110 - 114.

Background and Introduction: Li-ion battery

Si anode: Volume change problem



Electrode cracking



Before

After 5 cycles

Scrosati, B et al., Journal of Power Sources, 2010, 195,

Biomass silicon (Si): natural anode materials

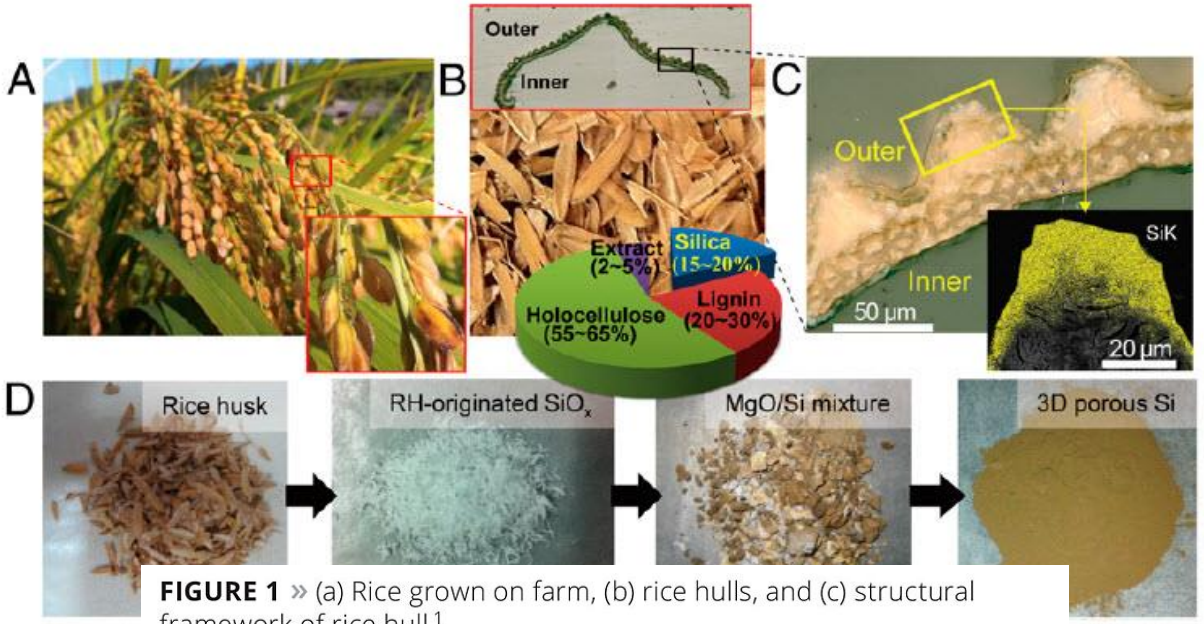
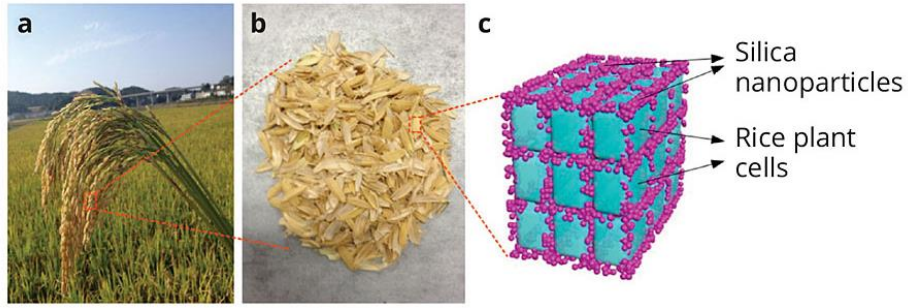


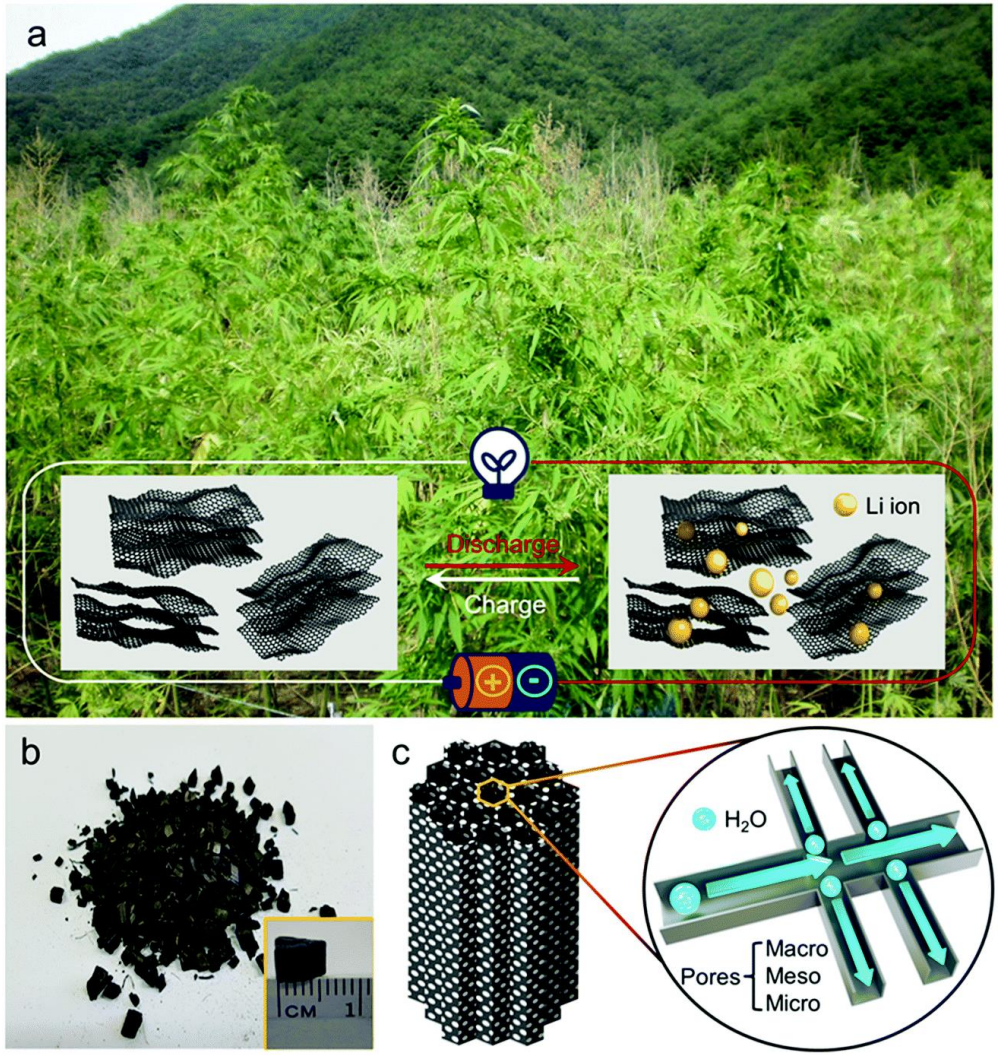
FIGURE 1 » (a) Rice grown on farm, (b) rice hulls, and (c) structural framework of rice hull.[1]

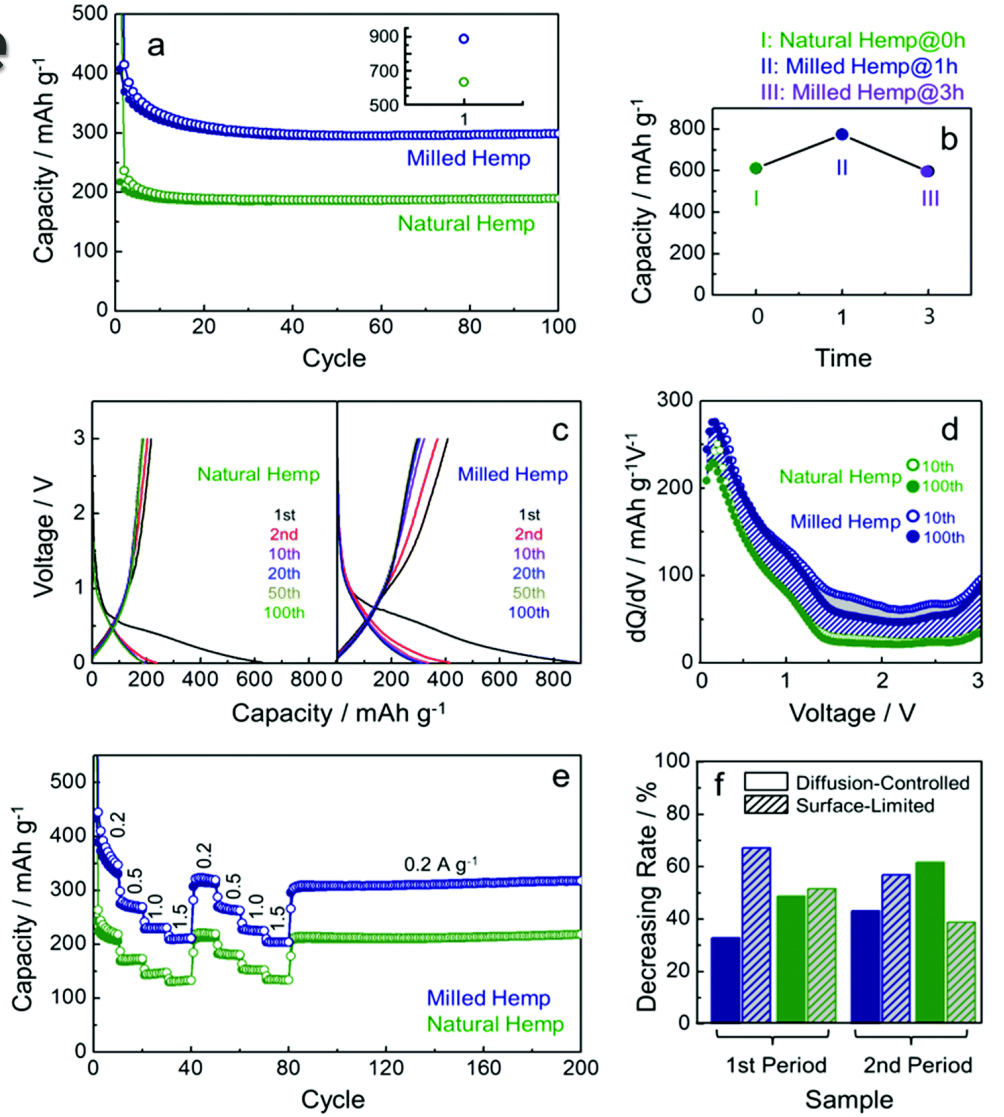


D.S. Jung, M.H. Ryon, Y.J. Sung, S.B. Park, J.W. Choi, PNAS 110 (2013) 12229-12234

BACKGROUND AND INTRODUCTION: Li-ion battery

Hemp-derived carbon for lithium storage





Electrochemical performance of natural hemp and milled hemp electrodes. (a) Cycling performance at a current density of 300 mA/g

Ji Hyun Um, et al., RSC Adv.,2018, 8, 32231–32240

Agricultural residues are an under-used carbon resource

1

Abundant and local

Rice, sugarcane, corn and fruit residues are generated in every ASEAN farming region; most are burned or landfilled.

2

Carbon-rich and tunable

Thermal conversion gives a carbon skeleton whose pores, surface groups and heteroatoms can be tuned by process conditions.

3

Low-cost and circular

Waste becomes a value-added material, cutting open burning and the need for fossil-derived carbons.

Biochar = carbon-rich solid from thermochemical conversion of biomass under limited oxygen; chemical activation turns it into high-surface-area porous carbon.

From biomass to functional carbon: a three-step toolbox

Conditions shown are those used in the popped-rice case study (Part 3).

STEP 1

Carbonization

Pyrolysis under N_2

Builds the aromatic carbon skeleton; volatiles leave



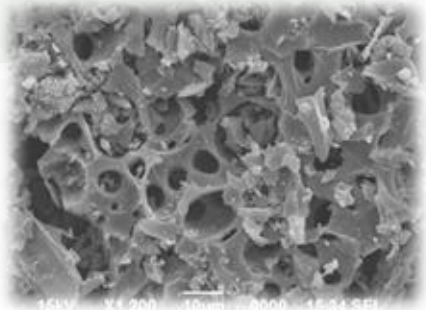
STEP 2

Activation

KOH etching

Opens micro- and mesopores; raises surface area

C : KOH = 1 : 2, 800 °C, 3 h; HCl wash



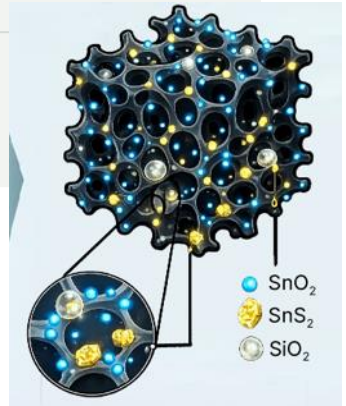
STEP 3

Functionalization

Hydrothermal loading

Adds active nanophases (metal oxides, sulfides) or magnetic phases

120–180 °C, 12–16 h

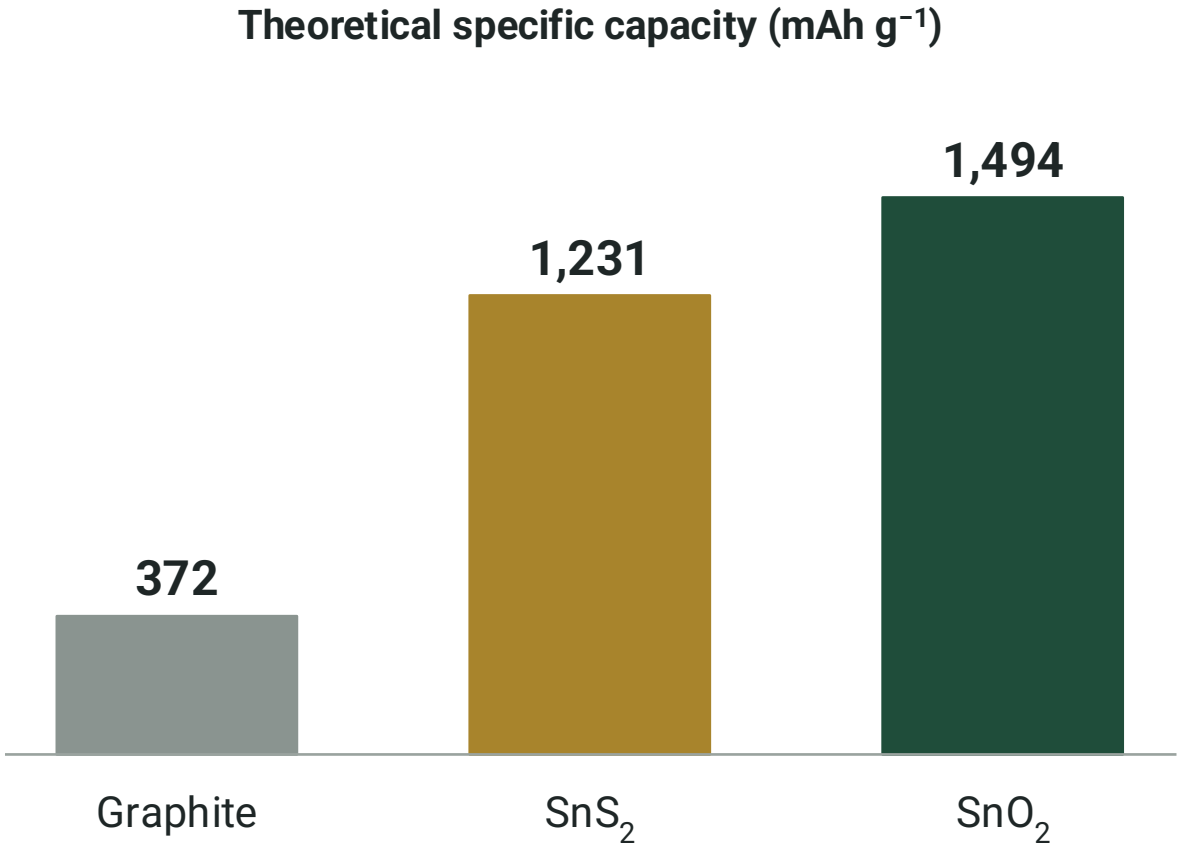


Same design rules serve remediation and energy

Material descriptor	Environmental remediation	Li-ion battery anode
High surface area, micropores	More adsorption sites, higher capacity	More Li^+ storage sites, but larger first-cycle SEI loss
Mesopores and macropores	Fast pollutant diffusion to inner sites	Electrolyte reservoirs, better rate capability
Surface O-groups	Affinity for polar and charged pollutants	Better electrolyte wetting; some irreversible capacity
Graphitic, conductive domains	π–π binding of aromatics	Electron transport to active nanophases
Inorganic content (e.g. SiO_2 from husk)	Usually removed or ignored	Extra Li-active phase when kept in a carbon matrix

One carbon platform, two jobs: what changes is the functional phase added on top.

Graphite limits the next generation of Li-ion anodes



1 Graphite

Low capacity (372 mAh g^{-1}), slow Li^+ diffusion, dendrite risk near 0 V

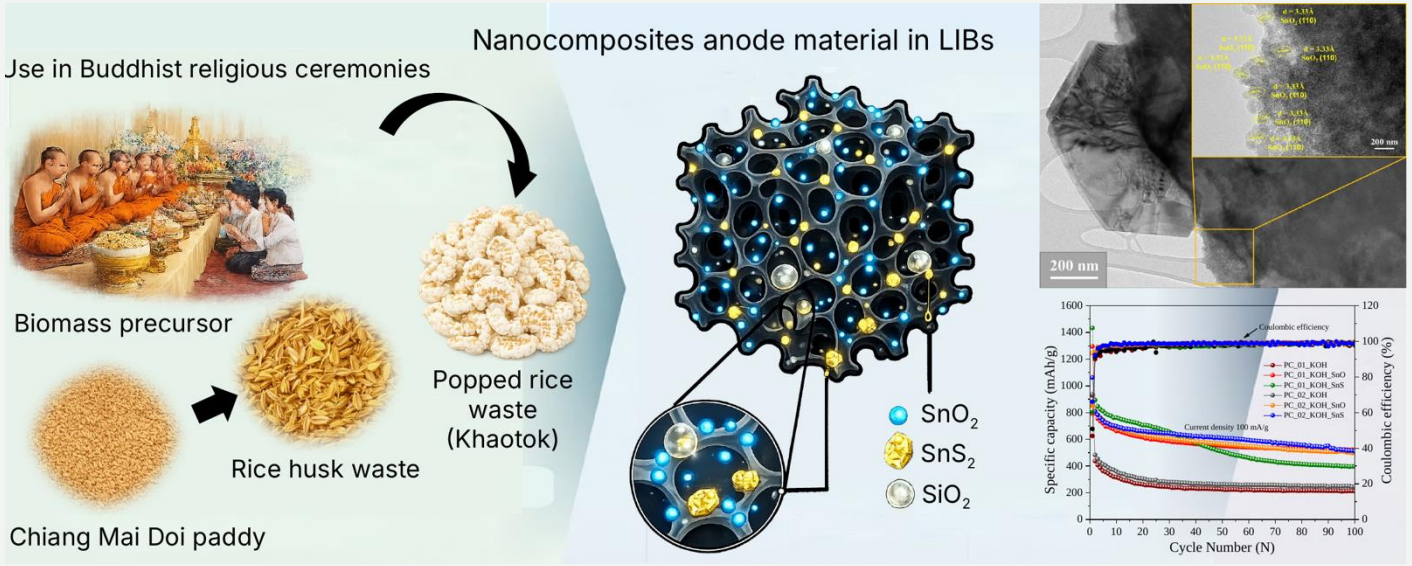
2 Sn-based phases

Conversion + alloying give 3–4 × graphite capacity, but volume change and aggregation cause fading

3 Strategy

Anchor Sn nanophases on a conductive, porous biomass carbon that buffers expansion

Khaotok: a culturally significant waste stream



Data: K. Pimta, T. Autthawong, W. Yodying, M. Haruta, T. Sarakonsri, Y. Chimupala, manuscript (2026)

SOURCE

Popped rice (khaotok) is offered in Buddhist ceremonies in Thailand and Southeast Asia and left over in large volumes

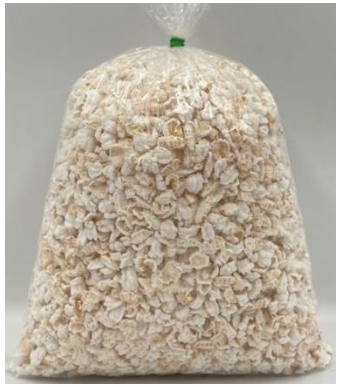
RAW MATERIAL

Doi paddy from Chiang Mai, popped in 1–2 min as trapped steam bursts the grain through the husk

TWO WASTES, TWO ROLES

Popped rice → porous carbon; rice husk → silica-containing carbon





Synthesis route and sample design

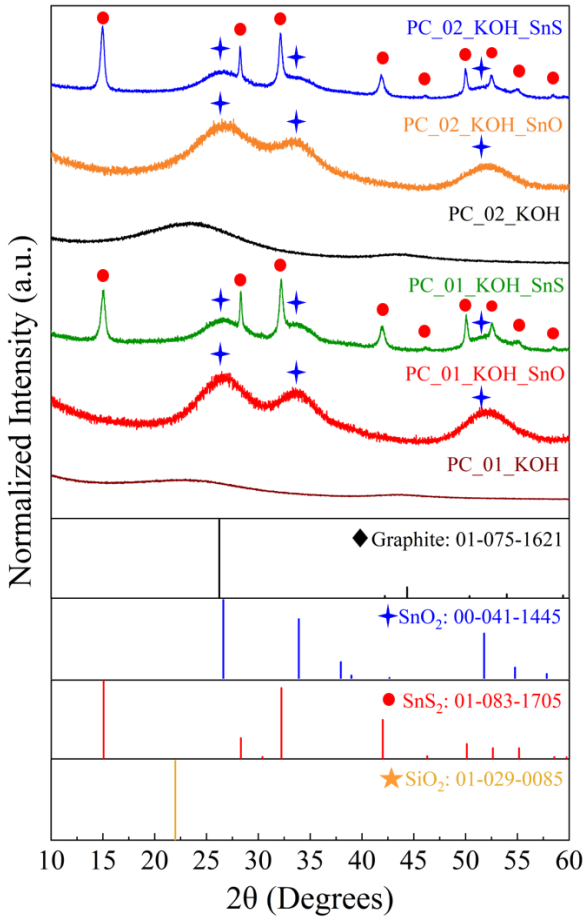
Popped rice (± rice husk) → **Carbonize 500 °C, N_2** → **KOH activation 800 °C, 3 h** → **Hydrothermal Sn loading**

Precursor	Activated carbon	+ SnO_2 quantum dots pH 8, 120 °C, 12 h	+ SnO_2/SnS_2 (L-cysteine) pH 8, 180 °C, 16 h
Popped rice only (PC_01)	PC_01_KOH	PC_01_KOH_SnO	PC_01_KOH_SnS
Popped rice + husk (PC_02)	PC_02_KOH	PC_02_KOH_SnO	PC_02_KOH_SnS

Electrodes: 70 wt% active material, 15 wt% Super-P, 15 wt% sodium alginate on Cu foil; CR2016 half-cells vs Li, 1 M $LiPF_6$ in EC/DMC (1 : 1), 0.01–3.00 V.

Data: K. Pimta, T. Autthawong, W. Yodying, M. Haruta, T. Sarakonsri, Y. Chimupala, manuscript (2026)

XRD: an amorphous carbon host for SnO_2 and SnS_2



Carbon matrix

Broad humps at 2θ ≈ 16–26° and 40–50°: mainly amorphous carbon with a minor graphitic component

Retained silica

PC_02 shows an extra broad amorphous SiO_2 feature near 23°, from the rice husk

SnO_2 quantum dots

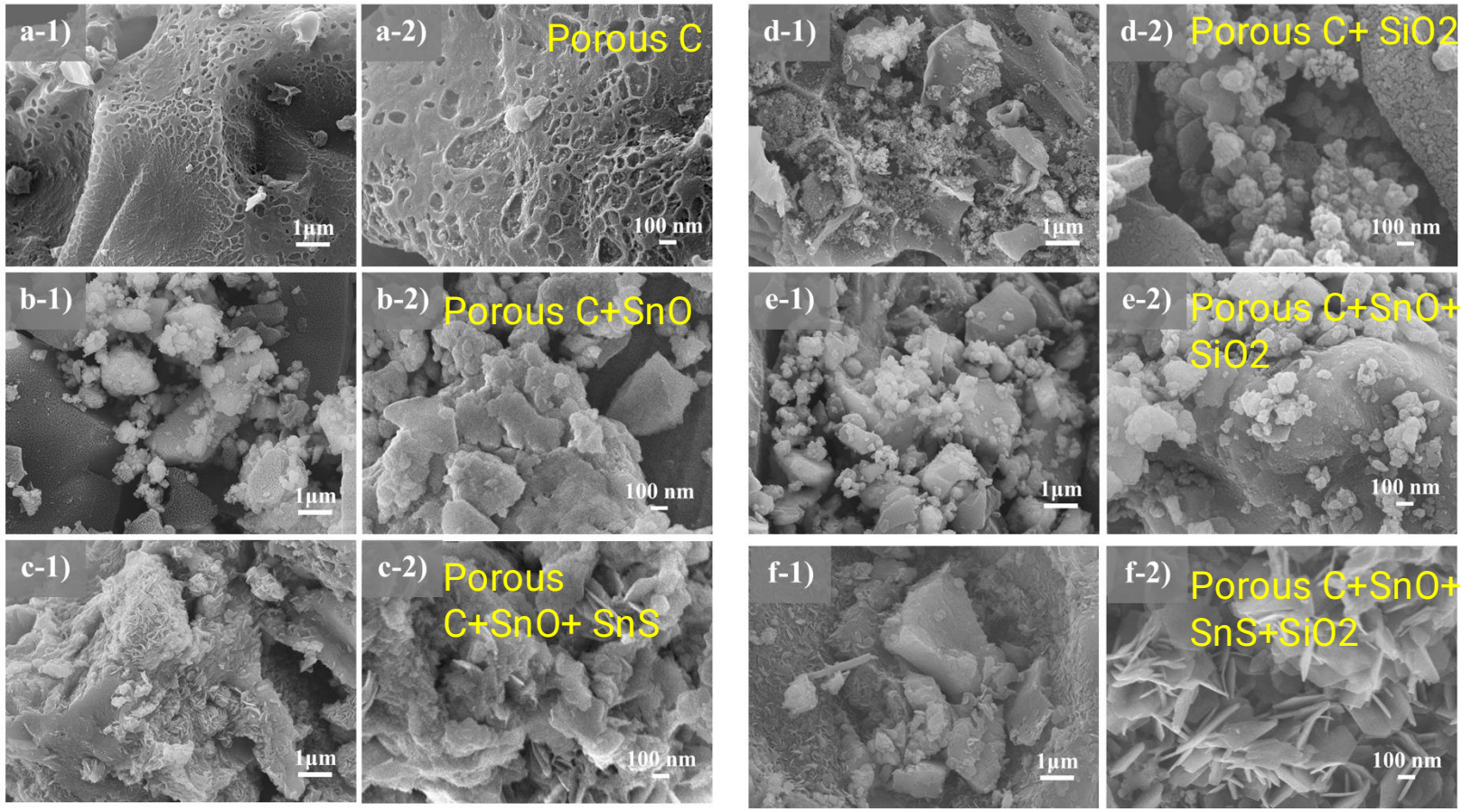
Very broad SnO_2 reflections indicate extremely small crystallites

SnS_2 phase

Sharp, strong SnS_2 reflections in the _SnS samples, alongside the broad SnO_2 pattern

Data: K. Pimta, T. Autthawong, W. Yodying, M. Haruta, T. Sarakonsri, Y. Chimupala, manuscript (2026)

Popping creates a 10 µm macroporous network



~10 µm

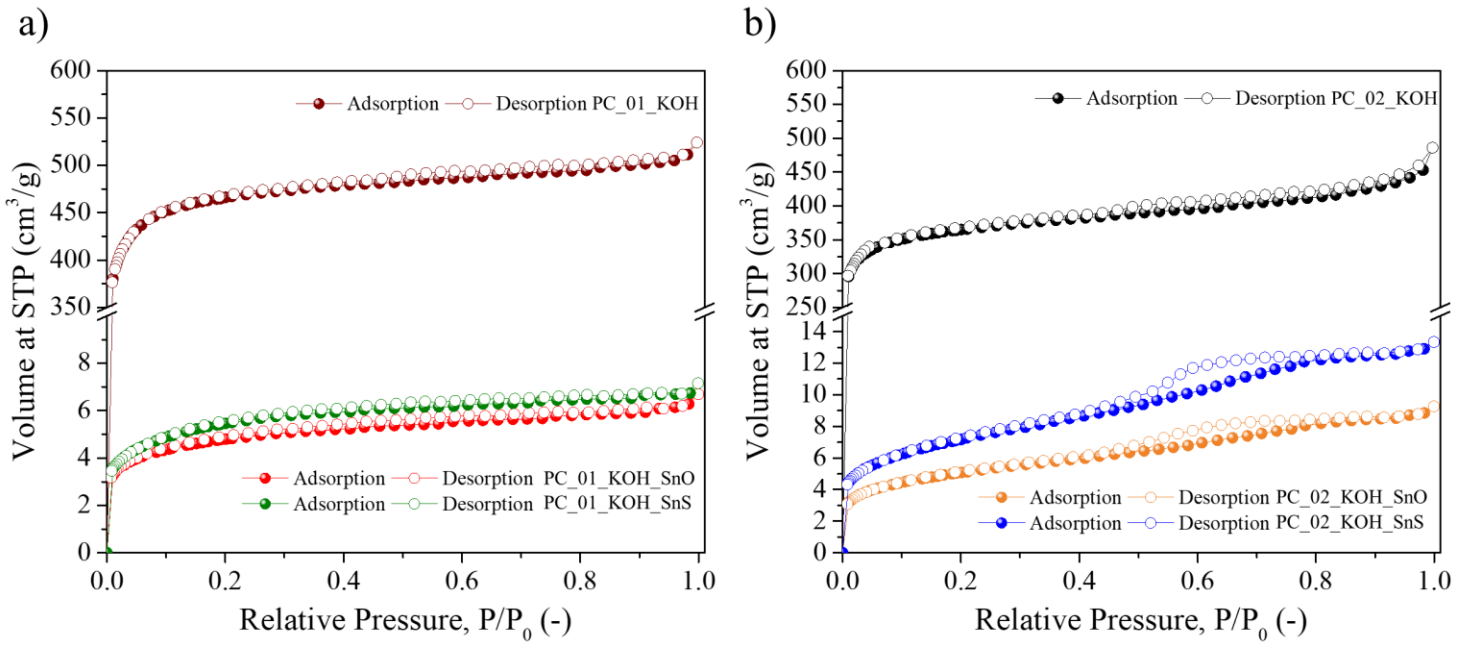
interconnected macropores in all PC samples

Formed when internal steam pressure in the grain is released instantly on popping — a built-in template, no additive needed.

(a) PC_01_KOH (b) _SnO (c) _SnS
(d) PC_02_KOH (e) _SnO (f) _SnS
1 = 10 000×, 2 = 50 000×

Data: K. Pimta, T. Autthawong, W. Yodying, M. Haruta, T. Sarakonsri, Y. Chimupala, manuscript (2026)

KOH activation delivers up to 2010 $m^2 g^{-1}$

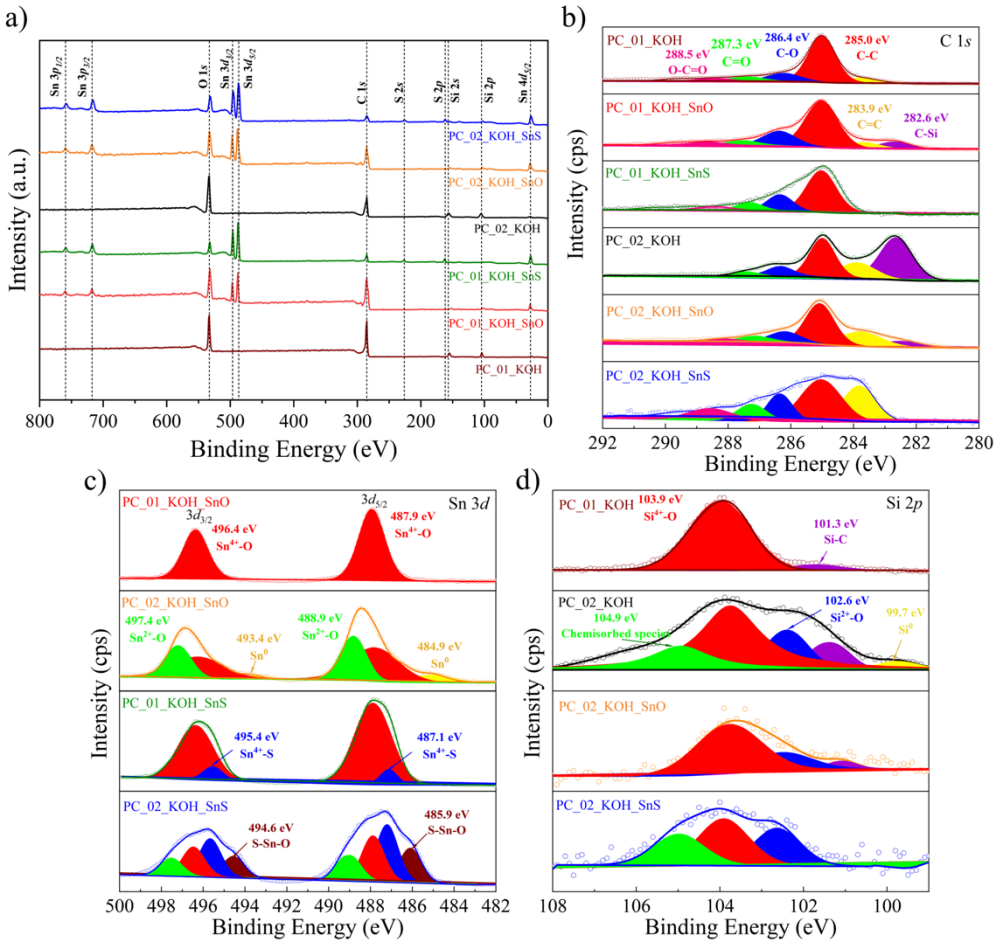


Sample	BET area ($m^2 g^{-1}$)	Pore vol. ($cm^3 g^{-1}$)
PC_01_KOH	1809	0.811
PC_01_KOH_SnO	1166	0.690
PC_01_KOH_SnS	**2010**	**1.117**
PC_02_KOH	1402	0.752
PC_02_KOH_SnO	823.8	0.646
PC_02_KOH_SnS	1007	0.806

- Type I behaviour for the pristine carbons: microporous activated carbon
- Hysteresis in the composites: mesopores that act as Li^+ reservoirs and aid rate capability
- SnO_2 loading partly fills pores; the SnS_2 route keeps or raises surface area

Data: K. Pimta, T. Autthawong, W. Yodying, M. Haruta, T. Sarakonsri, Y. Chimupala, manuscript (2026)

XPS confirms Sn–O, Sn–S and naturally retained silica



Survey — C and O in the pristine carbons; Si in husk-containing samples; Sn (and S) after loading

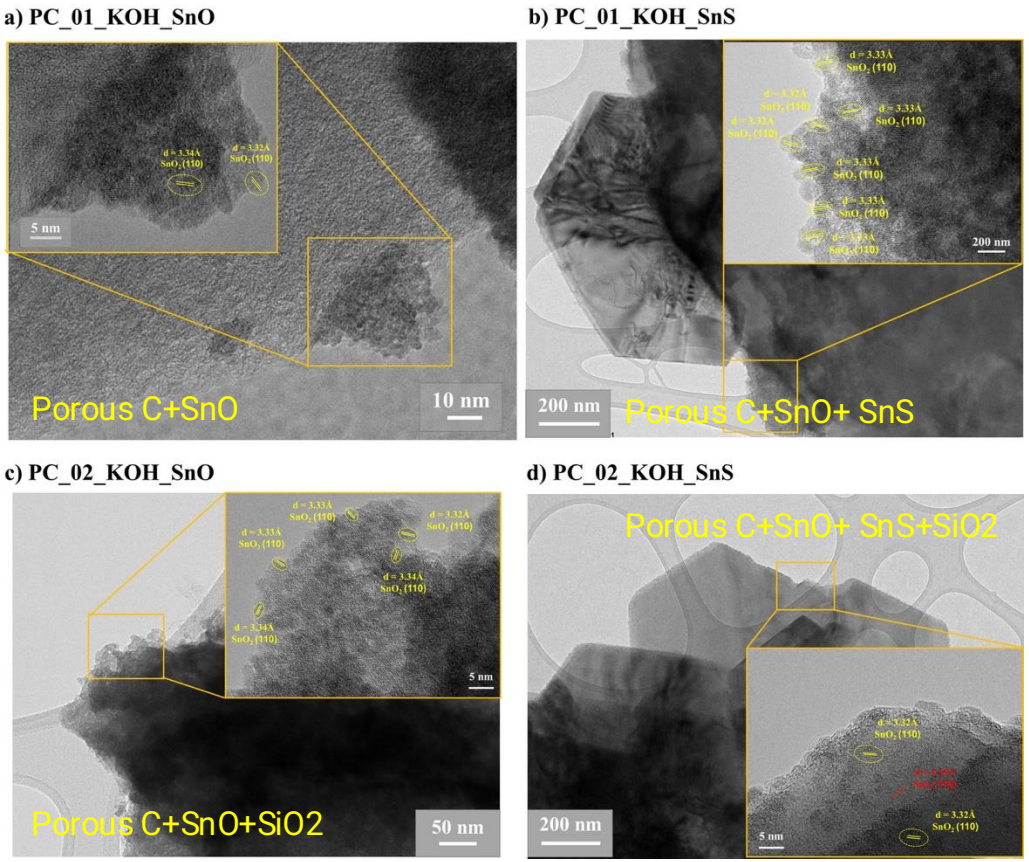
C 1s — C=C, C–C, C–O, C=O, O–C=O: conductive carbon plus O-groups that improve wetting; C–Si at 282.6 eV

Sn 3d — Sn^{4+}–O (487.9 / 496.4 eV) in SnO_2; Sn–S in SnS_2; mixed S–Sn–O at the oxide/sulfide interface

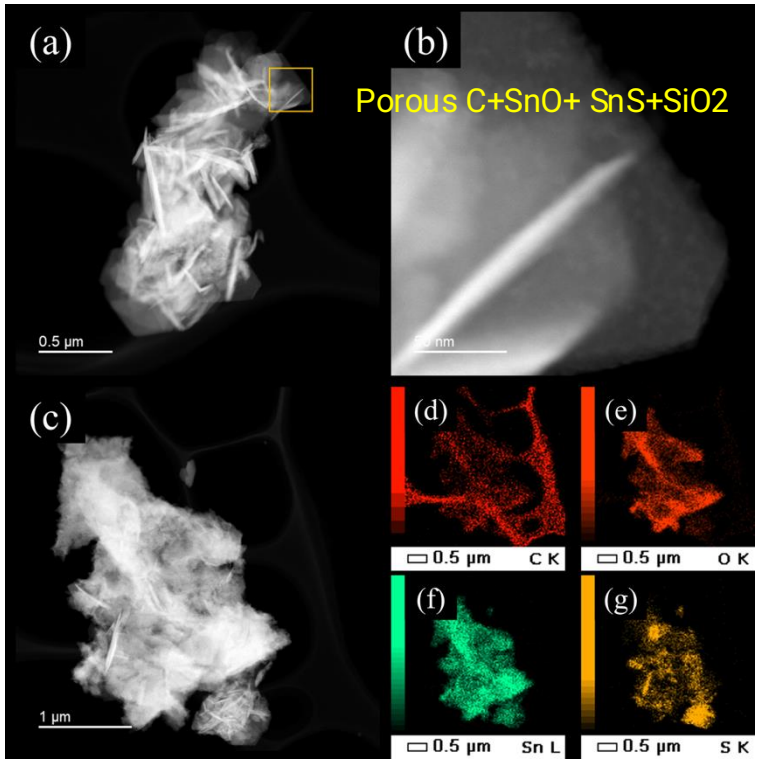
Si 2p — SiO_2 (103.9 eV) with Si–C; PC_02_KOH also shows Si^0 and SiO

Data: K. Pimta, T. Autthawong, W. Yodying, M. Haruta, T. Sarakonsri, Y. Chimupala, manuscript (2026)

SnO_2 quantum dots and SnS_2 sheets decorate the carbon



TEM / HRTEM of the four composites



STEM-EDS, PC_02_KOH_SnS (Fig. S2)

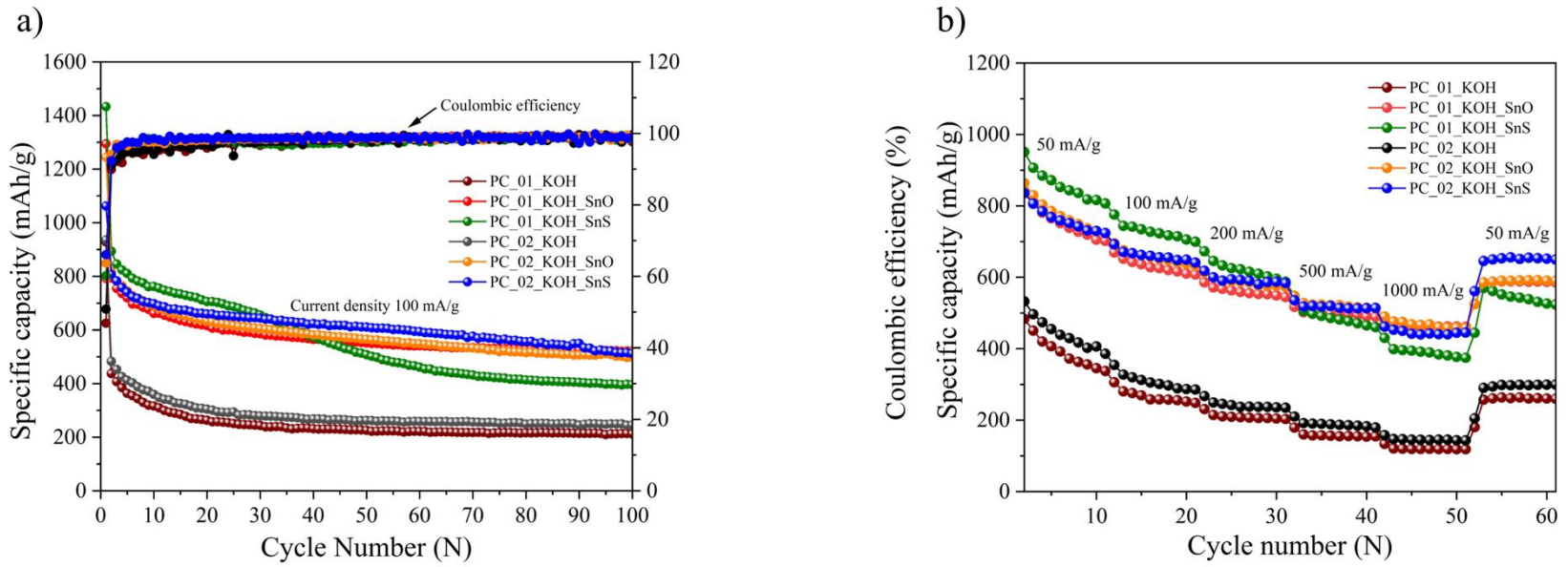
3.32–3.34 Å

d-spacing of SnO_2 (110) lattice fringes

Sn and S co-localize on the SnS_2 sheets; the C map is continuous

Data: K. Pimta, T. Autthawong, W. Yodying, M. Haruta, T. Sarakonsri, Y. Chimupala, manuscript (2026)

Sn nanophases more than double the reversible capacity



(a) Cycling, 100 mA g^{-1}

(b) Rate, 50–1000 mA g^{-1}

520.9 mAh g^{-1}

PC_01_KOH_SnO
vs 212.4 for PC_01_KOH

511.9 mAh g^{-1}

PC_02_KOH_SnS
vs 244.7 for PC_02_KOH

737.9 mAh g^{-1}

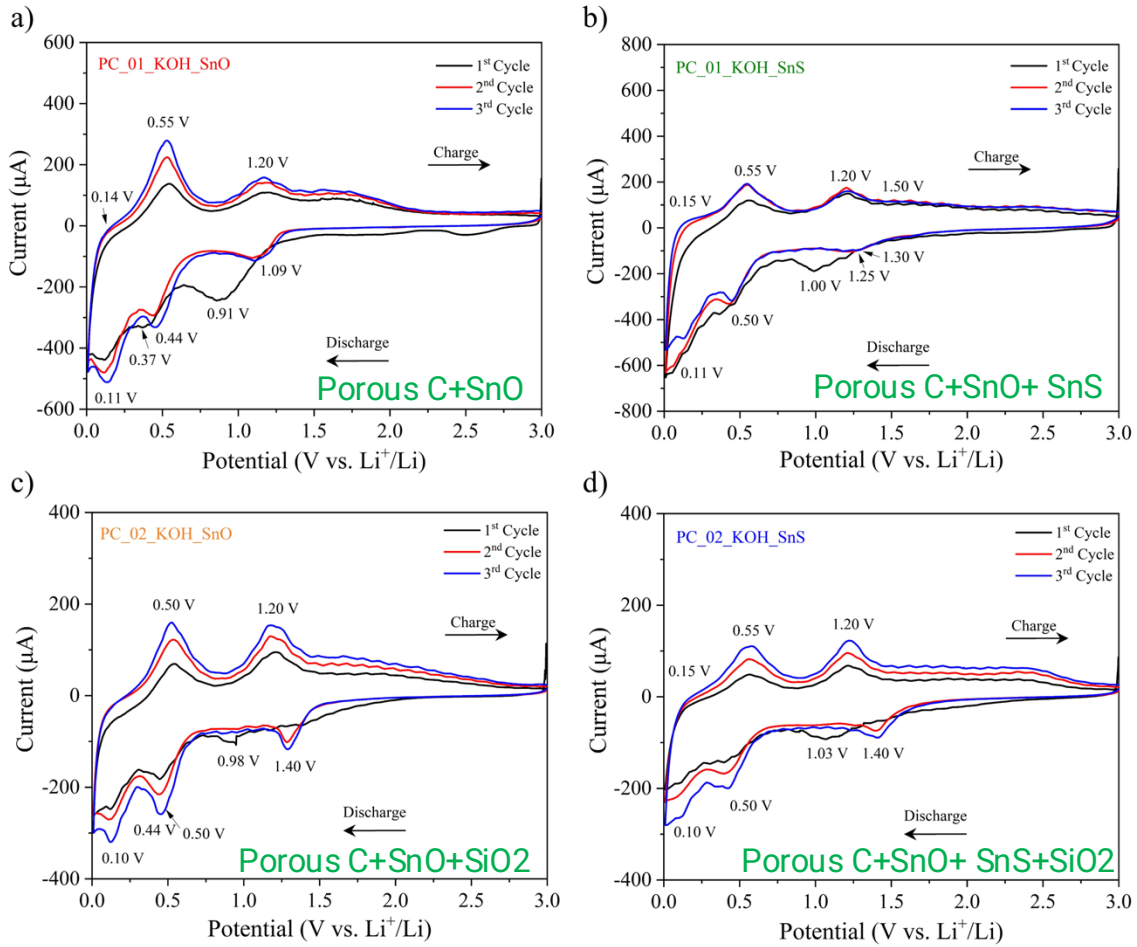
PC_02_KOH_SnS
recovered at 50 mA g^{-1} after 1000 mA g^{-1}

After 100 cycles

- First-cycle loss from SEI: ICE 47–66 %
- SiO_2 in PC_02 raises capacity of bare carbon (244.7 vs 212.4)
- SnS_2 gives the highest early capacity; SnO_2 the best stability

Data: K. Pimta, T. Autthawong, W. Yodying, M. Haruta, T. Sarakonsri, Y. Chimupala, manuscript (2026)

Cyclic voltammetry resolves each lithium-storage reaction

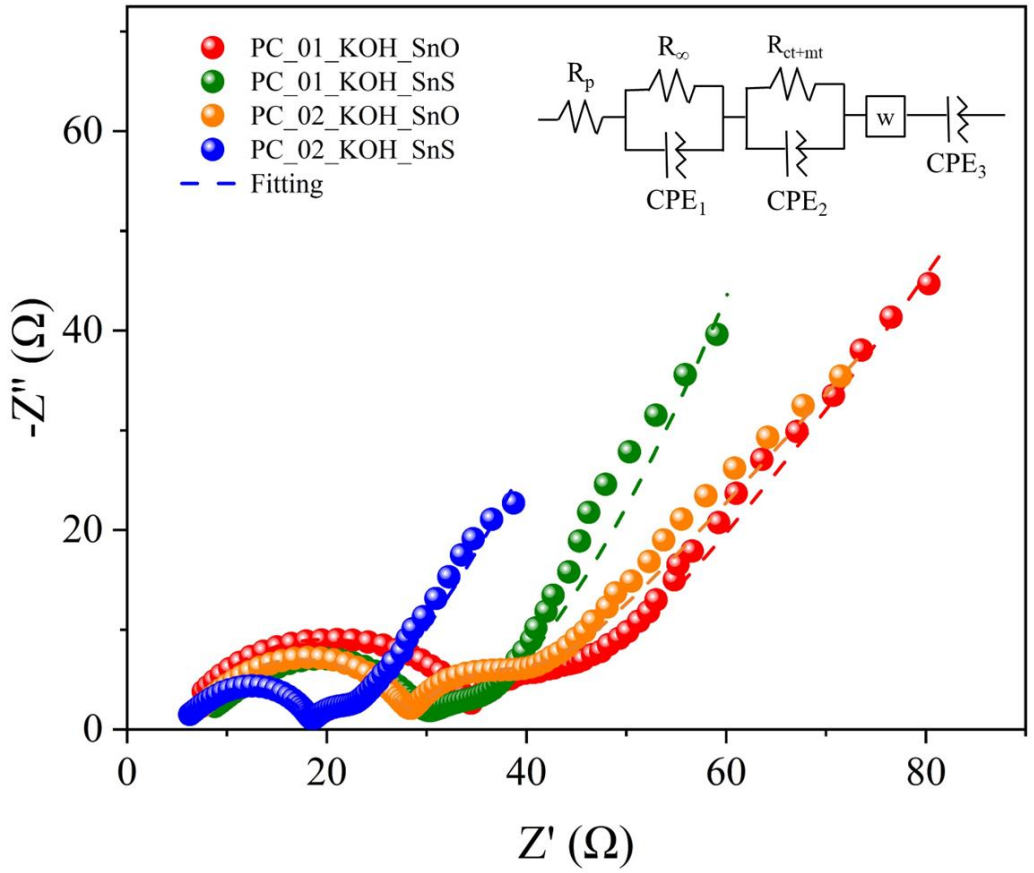


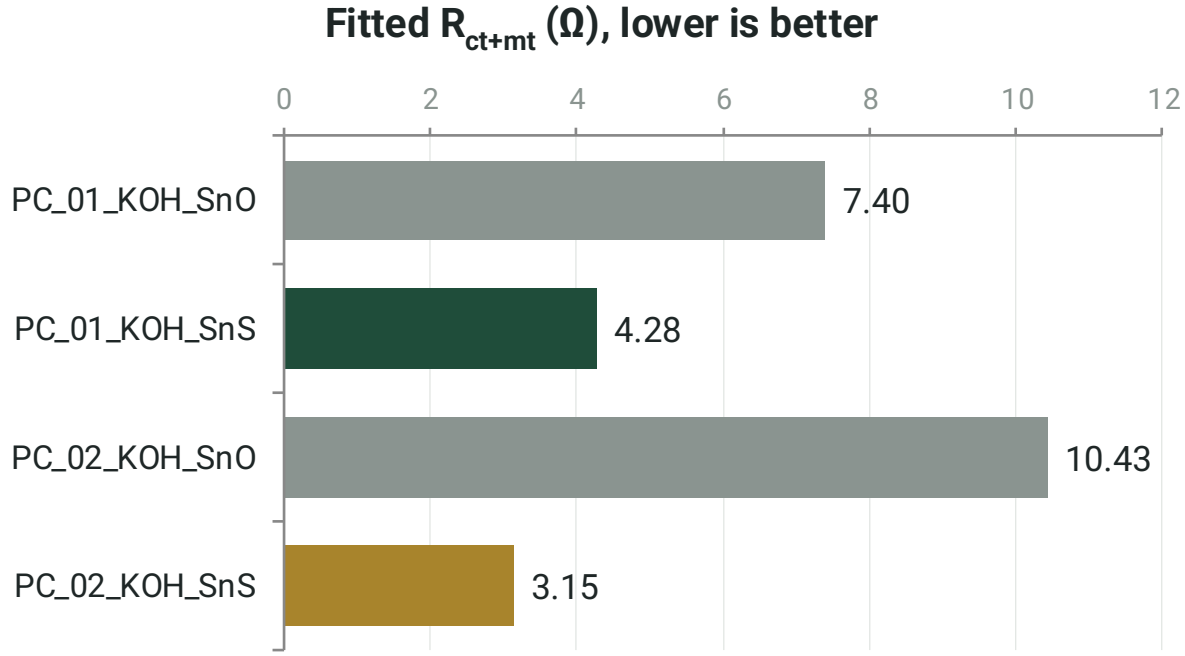
Data: K. Pimta, T. Autthawong, W. Yodying, M. Haruta, T. Sarakonsri, Y. Chimupala, manuscript (2026)

~1.0 V (1st scan)	$Li^+ + e^- +$ electrolyte → SEI
1.2 / 1.1 V	$SnO_2 + 4Li^+ + 4e^- \rightleftharpoons Sn + 2Li_2O$
1.3–1.5 V	$SnS_2 + 4Li^+ + 4e^- \rightleftharpoons Sn + 2Li_2S$
0.4–0.55 V	$Sn + xLi^+ + xe^- \rightleftharpoons Li_xSn \ (x \leq 4.4)$
~0.1 V	$6C + xLi^+ + xe^- \rightleftharpoons Li_xC_6$
PC_02 only	$SiO_2 + 4Li^+ + 4e^- \rightarrow 2Li_2O + Si;\ Si \rightleftharpoons Li_xSi$

PC_02: sharper 1.3 V anodic peak; Li_2O from SiO_2 may aid $Sn \rightarrow SnO_2$ reconversion

SnS_2 and retained SiO_2 lower the charge-transfer resistance





- SnS_2 lowers R_{ct+mt} in both series (7.40 → 4.28; 10.43 → 3.15 Ω)
- PC_02_KOH_SnS: lowest R_{ct+mt} and R_∞, highest ICE (66.1 %)

Data: K. Pimta, T. Autthawong, W. Yodying, M. Haruta, T. Sarakonsri, Y. Chimupala, manuscript (2026)

Performance of all six electrodes

Sample	BET area ($m^2\ g^{-1}$)	1st discharge (mAh g^{-1})	ICE (%)	After 100 cycles (mAh g^{-1})
PC_01_KOH	1809	928.1	46.9	212.4
PC_01_KOH_SnO	1166	1294.8	59.3	**520.9**
PC_01_KOH_SnS	2010	1433.1	60.2	396.3
PC_02_KOH	1402	935.9	50.8	244.7
PC_02_KOH_SnO	823.8	1244.6	63.7	498.8
PC_02_KOH_SnS	1007	1062.3	**66.1**	**511.9**

All at 100 mA g^{-1}, 0.01–3.00 V vs Li/Li^+. Gold = best in column.

Data: K. Pimta, T. Autthawong, W. Yodying, M. Haruta, T. Sarakonsri, Y. Chimupala, manuscript (2026)

From ceremony waste to battery anodes

1. Biomass carbon is a platform: carbonization, activation and functionalization tune it for remediation or energy storage

2. Popping is a free template: khaotok carbon reaches 1809 $m^2 g^{-1}$ after KOH activation, with ~10 µm macropores

3. SnO_2 quantum dots and SnO_2/SnS_2 raise capacity to 520.9 and 511.9 mAh g^{-1} after 100 cycles, 2.1–2.5× the bare carbons

4. Rice husk is not waste in the anode: retained SiO_2 adds Li storage and, with SnS_2, gives the lowest resistance

Acknowledgements

Co-authors

Korawith Pimta, Chiang Mai University

Thanapat Autthawong, Chiang Mai University

Waewwow Yodying, Chiang Mai University

Mitsutaka Haruta, ICR, Kyoto University

Prof.Dr.Thapanee Sarakonsri, Chiang Mai University

PTEM Lab and Renewable Energy Laboratory Research Group, Department of Industrial Chemistry, CMU

Funding and support

CMU Proactive Researcher Program (735/2567)

Fundamental Fund 2025, Chiang Mai University (207605)

Thailand Science Research and Innovation, TSRI (FRB680102/0162)

Center of Excellence for Innovation in Chemistry (PERCH-CIC), MHESI

ICR International Collaborative Research Program, Kyoto University (2025-136)

Thank you

Asst. Prof. Dr. Yothin Chimupala

Department of Industrial Chemistry, Faculty of Science

Chiang Mai University, Thailand

yothin.chimupala@cmu.ac.th

